Available online at www.sciencedirect.com
ScienceDirect
Ceramics International 34 (2008) 1139–1144
CERAMICS INTERNATIONAL
www.elsevier.com/locate/ceramint

Biomimetic apatite deposited on microarc oxidized anatase-based ceramic coating

Daqing Wei, Yu Zhou *, Dechang Jia, Yaming Wang

Institute for Advanced Ceramics, Harbin Institute of Technology, Harbin 150001, PR China

Received 7 November 2006; received in revised form 11 December 2006; accepted 2 February 2007
Available online 6 March 2007

Abstract

Biomimetic apatite was formed on a microarc oxidized (MAO) anatase-based coating containing Ca and P in a simulated body fluid (SBF). At the process of the SBF immersion (0–96 h), the Ca and P of the MAO coating dissolve into the SBF, increasing the supersaturation degree near the surface of the MAO coating, which could promote the formation and growth of apatite. After SBF immersion for 7 days, the surface of the MAO coating was modified slightly. The entire surface immersed for 14 days was covered by an apatite coating. The apatite possesses carbonated structure, controllable crystallinity and pore networks. The results indicate that the MAO coating formed in an electrolyte containing phosphate and EDTA–Ca chelate complex possesses good apatite-forming ability.

Keywords: B. Surfaces; D. TiO_2; Microarc oxidation; Biomimetic apatite

1. Introduction

Hydroxyapatite and bioactive glass–ceramic both exhibit good bioactivity [1–3]. Unfortunately, these bioactive ceramic materials are not suitable for load-bearing conditions on account of their poor mechanical properties [4]. Titanium and its alloys have been used widely as load-bearing implants (e.g., skeletal repair and dental implants) due to their excellent mechanical toughness, strength, biocompatibility and corrosion resistance [5]. However, they exhibit poor osteoinductive properties because of their bioinert character [5]. To improve their bioactivity, many surface modifying techniques, such as plasma spraying [6–8], sol–gel method [9,10] and electrophoresis and electrochemical deposition [11,12], have been developed to prepare bioactive ceramic coatings on titanium and its alloys. Among these techniques, plasma spraying is currently used to fabricate HA coating. However, the decomposition of HA occurs unavoidably because of a high temperature during deposition process [7]. Moreover, the interfacial bonding between HA coating and substrate is not very strong [8]. Additionally, this technique is not suitable to prepare uniform coatings on biomedical implants with complex geometries.

Plasma electrochemical method, microarc oxidation (MAO), is a relatively convenient and effective technique to deposit ceramic coatings on the surfaces of Ti, Al, Mg and their alloys [13]. This technique can produce various functional coatings with a porous structure and various desired constituents can be introduced into TiO_2 coating [14–16]. Moreover, it is very suitable to modify various substrates with complex shapes. Additionally, MAO ceramic coatings usually exhibit good interface bonding with substrates. In recent years, using MAO technique to deposit bioactive ceramic coatings on titanium and its alloys has received considerable attention [14–19]. To prepare bioactive coatings on titanium and its alloys, introductions of Ca and P elements into MAO coatings are taken into account. In the previous studies, various calcium salts such as calcium acetate, calcium glycerophosphate and calcium dihydrogen phosphate were used in MAO process [14–19]. In this work, apatite-forming ability of the MAO coating formed in an electrolyte containing phosphate, Ca–EDTA chelate complex, etc., was reported.

* Corresponding author at: Department of Materials Science and Engineering, Harbin Institute of Technology, P.O. Box 433, Harbin 150001, PR China. Tel.: +86 451 8641 5898; fax: +86 451 8641 4291.
E-mail address: ce921@hit.edu.cn (Y. Zhou).

0272-8842/$34.00
doi:10.1016/j.ceramint.2007.02.009

2. Experimental

2.1. Samples preparation

Ti6Al4V plates (10 mm × 10 mm × 1.5 mm) were used as anodes, and stainless steel plates were used as cathodes in an electrolytic bath. The plates were ground with abrasive papers, ultrasonically washed with acetone and deionized water, and dried at 40 °C. An fresh electrolyte was prepared by dissolving reagent-grade chemicals of $Ca(CH_3COO)_2{\cdot}H_2O$ (6.3 g/l), $Ca(H_2PO_4)_2{\cdot}H_2O$ (13.2 g/l), EDTA–2Na (15 g/l) and NaOH (15 g/l) into deionized water. In the MAO process, the applied voltage, frequency, duty cycle and oxidizing time were 300 V, 600 Hz, 8.0% and 5 min, respectively. The temperature of the electrolyte was kept at 40 °C by a cooling system.

2.2. SBF immersion of the samples

The MAO samples were soaked in 15 ml SBF with ionic concentrations nearly equal to those of human blood plasma ([20], Table 1), and the SBF was refreshed every other day. The SBF was prepared by dissolving reagent-grade chemicals of NaCl, $NaHCO_3$, KCl, $K_2HPO_4{\cdot}3H_2O$, $MgCl_2{\cdot}6H_2O$, $CaCl_2$, and Na_2SO_4 into deionized water and buffering at pH 7.40 with tris-hydroxymethyl-aminomethane ($(CH_2OH)_3CNH_2$) and 1.0 mol/l HCl at 37 °C.

2.3. Analyses of the structure and phase composition

The phase composition of the surfaces of the MAO samples before and after soaking in the SBF were analyzed by Glance-angle X-ray diffraction (GA-XRD, Philips X'Pert, Holland) using a Cu Kα radiation. In the GA-XRD experiment, the angle of the incident beam was fixed at 1° against the surface of the sample and the measurements were performed with a continuous scanning mode at a rate of 2°/min.

An X-ray photoelectron spectroscopy (XPS, PHI 5700, America physical electronics) was used to determine the chemical composition of the surface of the MAO coating. In the XPS experiment, an Al Kα (1486.6 eV) X-ray source was used with an anode powder of 250 W (12.5 kV, 20 mA) for the XPS work. The XPS take-off angle was set at 45°, detecting the depth range of 5–10 nm. The region of 2 mm × 0.8 mm on the surface of the sample was analyzed with a hemispherical analyzer. The measured binding energies were calibrated by the C 1s (hydrocarbon C–C, C–H) of 285 eV.

A scanning electron microscopy (SEM, CamScan MX2600, CamScan Co., England) was used to observe the surface morphologies of the MAO coatings after SBF immersion.

Fourier transform infrared spectroscopy (FT-IR, Bruker Vector 22, Germany) was used to analyze the phase and structure of the MAO coating after SBF immersion. In the FT-IR experiment, the scanning range and resolution were 4000–400 and 4 cm^{-1}, respectively. Approximately 1 mg of the coating on the SBF-treated MAO sample was removed from the substrate, mixed with about 500 mg of dry KBr powder and ground using an agate mortar and pestle. The mixed and ground powder was pressed into transparent disks with a diameter of 13 mm for the FT-IR work.

Ca and P concentrations of the SBF with immersion of the MAO coating for 0, 24, 48, 72 and 96 h were measured by an inductively coupled plasma optical emission spectroscopy (ICP-OES, Optima 5300DV, Perkin-Elmer, America). In the ICP-OES measurement, the ion concentrations of 10 ml SBF after immersion of one sample with surface area of 10 mm × 10 mm were measured, and two independent analyses were carried out for each solution.

Table 1
Ion concentrations of the SBF and human blood plasma

Ion	Concentration (mmol/l)	
	SBF	Blood plasma
Na^+	142.0	142.0
K^+	5.0	5.0
Mg^{2+}	1.5	1.5
Ca^{2+}	2.5	2.5
Cl^-	147.8	103.8
HCO_3^{2-}	4.2	27
HPO_4^{2-}	1.0	1.0
SO_4^{2-}	0.5	0.5

3. Results

3.1. Structure of the MAO coating

The XRD pattern of the surface of the MAO coating is shown in Fig. 1. A weak diffraction peak at $2\theta = 25.3°$ and diffraction at $2\theta = 22.5–40°$ were observed on the surface of the MAO coating, suggesting the presences of anatase with low crystallinity and amorphous phase.

The XPS results of the MAO coating show that the surface of the MAO coating mainly contains Ti, Ca, P, C and O (Fig. 2a). No N and V were detected on the surface of the MAO coating. The Ca and P concentrations are about 11.1 and 6.1 at.% with Ca/P about 1.8. The values of the binding energies (BE) of Ti $2p_{3/2}$ and Ti $2p_{1/2}$ are 458.3 and 464.4 eV corresponding to a

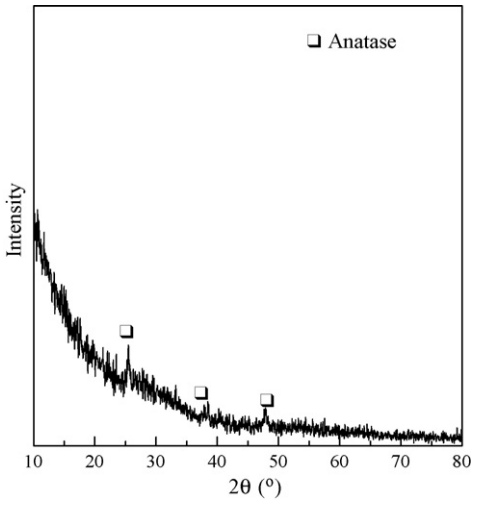

Fig. 1. XRD pattern of the MAO coating.

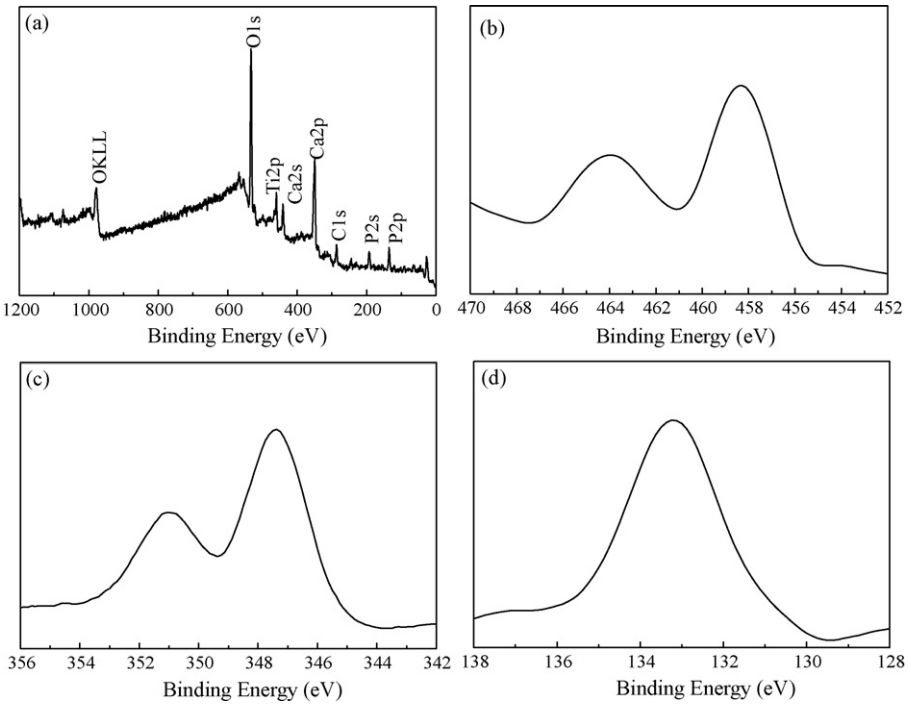

Fig. 2. XPS spectra of the MAO coating: (a) XPS survey, (b) Ti 2p, (c) Ca 2p and (d) P 2p.

chemical state of Ti^{4+} (Fig. 2b), which are typical BE for TiO_2 according to the reported results [14]. The Ca 2p spectrum of the MAO coating reveals a doublet with Ca $2p_{3/2}$ (BE of 347.4 eV) and Ca $2p_{1/2}$ (BE of 351.0 eV) (Fig. 2c), corresponding to the presence of Ca^{2+} [16]. The P 2p spectrum of the MAO coating reveals a single peak at BE position of 133.3 eV (P $2p_{3/2}$) (Fig. 2d), indicating the presence of P^{5+} according to published data [14,16].

The surface morphology of the surface of the MAO coating is shown in Fig. 3. The MAO coating exhibits a porous structure, which is beneficial to cell attachment, propagation and bone growth [15]. As can be seen, the micropores with diameters ~5 μm are distributed at regular intervals.

3.2. Biomimetic apatite on the MAO coating

The surface morphologies of the MAO coating after soaking in the SBF for 7 and 14 days are shown in Fig. 4. After 7 days, the surface of the MAO coating was modified slightly and the porous structure of the initial MAO coating can be distinguished (Fig. 4a). Further increasing the SBF immersion time to 14 days, the entire surface of the MAO coating was covered a new coating (Fig. 4b). Moreover, numerous sphere-like precipitates with diameters ~5 μm were observed. At a higher magnification, it was found that the new coating possesses a network structure mainly composed of nano-scale crystals with sizes of ~100 nm (Fig. 4c).

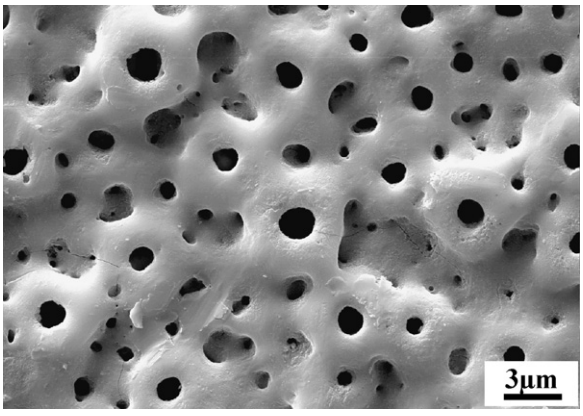

Fig. 3. SEM micrograph of the surface of the MAO coating.

The XRD patterns of the MAO coating after soaking in the SBF for 7, 14 and 28 days are shown in Fig. 5. After 7 days, no obvious diffraction peaks of the precipitates were observed on the surface of the SBF-treated MAO coating (Fig. 5a). After SBF immersion for 14 days, the diffraction peaks of apatite with poor crystallinity were observed (Fig. 5b). Further increasing the SBF immersion time to 28 days, the diffraction peaks of apatite increase (Fig. 5c). It is suggested that the crystallinity of biomimetic apatite can be controlled by immersion time in the SBF.

The FT-IR spectrum of the MAO coating after soaking in the SBF for 28 days is shown in Fig. 6. A broad absorption band at 3456 cm^{-1} and a bending mode at 1650 cm^{-1} are attributed to H_2O in the SBF-treated MAO coating. The spectrum clearly illustrate the triply degenerated asymmetric stretching modes of ν_3PO_4 bands at 1032 cm^{-1}, triply degenerated bending mode of ν_4PO_4 bands at 604 and 565 cm^{-1} and double degenerated bending mode of ν_2PO_4 bands at 472 cm^{-1} [21,22]. In the FT-IR spectrum, the CO_3^{2-} absorption bands also were observed including bending mode of the $\nu_4CO_3^{2-}$ group in A-type carbonated HA (CHA) at 1550 cm^{-1}, characteristic stretching mode of $\nu_3CO_3^{2-}$ group in CHA at 1508 cm^{-1}, characteristic stretching mode of $\nu_1CO_3^{2-}$ group in A-type CHA at 1562 cm^{-1}, stretching mode of $\nu_1CO_3^{2-}$ group in B-type

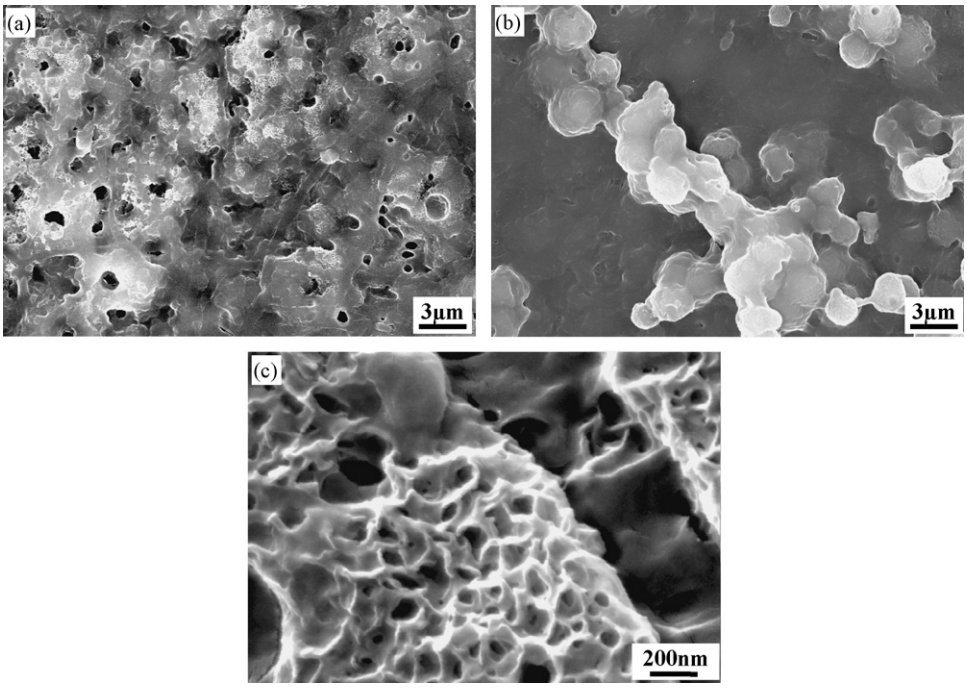

Fig. 4. SEM micrographs of the surfaces of the MAO coatings after soaking in the SBF: (a) 7 days, (b) 14 days and (c) higher magnification of (b).

CHA at 1426 cm^{-1} and bending mode of (ν_3 or ν_4) CO_3^{2-} group in CHA at 873 cm^{-1} [21,22]. In addition, the characteristic peaks at 1104, 956 and 873 cm^{-1} also suggest the presence of HPO_4^{2-} in the apatite, according to the reported results [21,22]. Additionally, OH^- stretch band in the FT-IR spectrum at 3560 cm^{-1} is not pronounced probably due to that the partial OH^- groups are substituted by the CO_3^{2-} groups (A-type substitution) during the apatite formation process. The results indicate that the MAO coating can induce the formation of carbonated apatite.

The XPS spectra of Ca 2p and P 2p of the MAO coating after SBF incubation for 14 days are shown in Fig. 7. The Ca 2p spectrum shows a doublet at 346.7 and 350.3 eV and P 2p spectrum reveals a single peak at 133.0 eV. These BE values are agree well with the previous results of carbonated HA obtained by biomimetic method [16].

Ca and P concentrations of the SBF with immersion of the MAO coating for 0–96 h are shown in Fig. 8. It can be seen that the Ca and P concentrations of the SBF increase continuously during the testing process (0–96 h). The results indicate that the Ca and P of the MAO coating can dissolve into the SBF.

4. Discussion

In this study, anatase-based coating containing Ca and P was formed on titanium alloy by MAO process in an electrolyte containing phosphate and EDTA-Ca. During the process of the electrolyte preparation, a chemical reaction between Ca^{2+} and H_2Y^{2-} ions occurs, showing in the following equation [14]:

$$Ca^{2+} + H_2Y^{2-} \leftrightarrow [CaY^{2-}] + 2H^+ \quad (Y = [_2(OOCCH_2)NCH_2CH_2N(CH_2COO)_2]^{4-}) \tag{1}$$

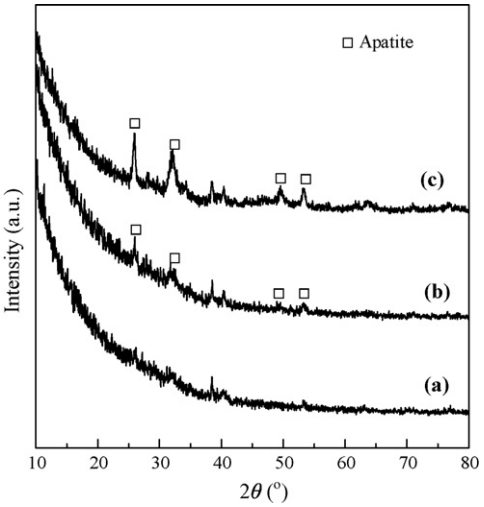

Fig. 5. XRD patterns of the MAO coatings after soaking in the SBF: (a) 7 days, (b) 14 days and (c) 28 days.

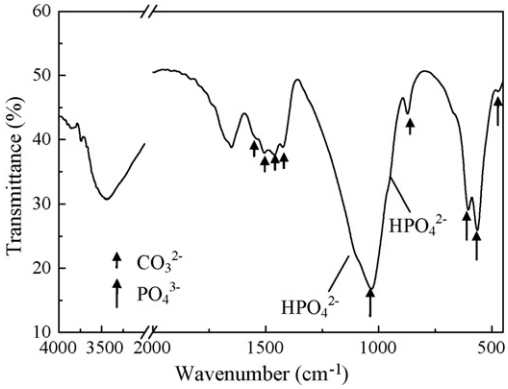

Fig. 6. FT-IR spectrum of the MAO coating after soaking in the SBF for 28 days.

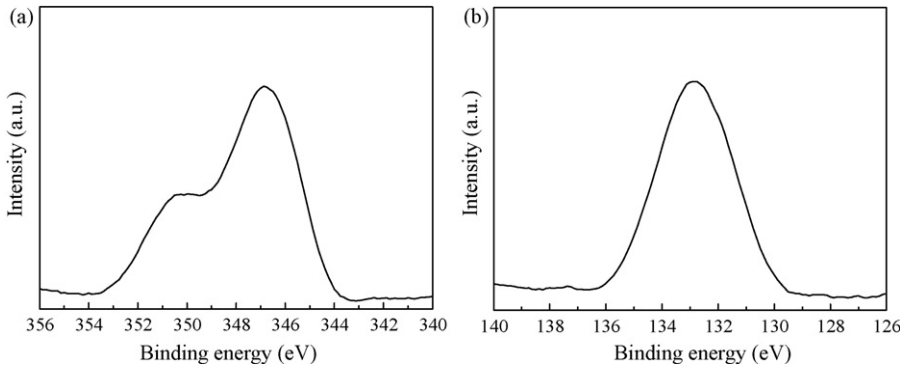

Fig. 7. XPS spectra of (a) Ca 2p and (b) P 2p of the surface of the MAO coating after SBF immersion for 14 days.

The negatively charged CaY^{2-} ions move to the anode easily in the electrolyte under the applied electrical field. The presence of the CaY^{2-} chelate complex is dependent on the stable chelate action of –N ↔ Ca ↔ OOCR–. If the –N ↔ Ca ↔ OOCR– structure exists in the MAO coating, the N could be detected by XPS. However, no N was found on the surface of the MAO coating. It is therefore reasonable to assume that the chemical band of N ↔ Ca was broken due to a high temperature condition on the anode surface during the MAO process [13]. Eventually, the N-containing organic compound was expelled from the MAO coating and the Ca would be released from the –N ↔ Ca ↔ OOCR– due to the thermal impact.

Biomimetic apatite was formed on the MAO coating containing Ca and P. The FT-IR, SEM and XRD results indicate that the apatite induced by the MAO coating possesses some important characters such as carbonated structure, controllable crystallinity and pore networks on the nanometer scale. In this study, the anatase-based coating containing Ca and P formed in the electrolyte containing phosphate and EDTA–Ca chelate complex exhibits good apatite-forming ability. The important aspect promoting the apatite formation may be associated with the dissolutions of Ca and P in this work. The ICP-OES results indicate the Ca and P of the MAO coating can be released into the SBF. By increasing immersion time, the supersaturation degree of the SBF with respect to apatite near the surface of the MAO coating occurs, which triggers the apatite nucleation. Once the apatite nuclei were formed, they could grow spontaneously by assembling the remaining calcium, phosphate and carbonic acid ions around apatite nuclei in the SBF.

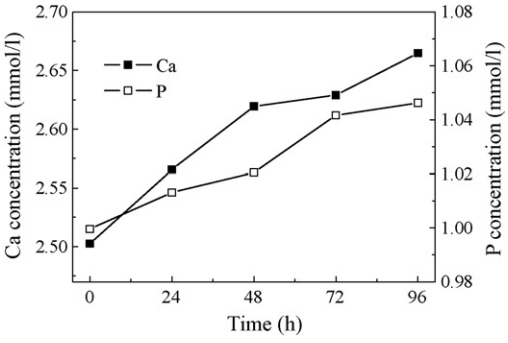

Fig. 8. Ca and P concentrations of the SBF with immersion of the MAO coating measured as a function of the SBF immersion time.

5. Conclusions

Anatase-based coating containing Ca and P on Ti6Al4V was prepared by microarc oxidation (MAO) in an electrolyte containing phosphate and EDTA–Ca. After SBF immersion for 14 days, the entire surface of the MAO coating was covered by a biomimetic apatite coating. The induced biomimetic apatite possesses some important characters such as carbonated structure, controllable crystallinity and pore networks on the nanometer scale. At the early stage of the SBF immersion (0–96 h), Ca and P of the MAO coating are released into the SBF, increasing the supersaturation degree near the surface of the MAO coating and further promoting the formation and growth of apatite.

References

[1] M. Wang, Developing bioactive composite materials for tissue replacement, Biomaterials 24 (2003) 2133–2151.
[2] S.K. Kalpana, Biomaterials in total joint replacement, Colloids Surf. B: Biointerf. 39 (2004) 133–142.
[3] D.A. Yang, Z. Yang, X. Li, L.-Z. Di, H. Zhao, A study of hydroxyapatite/calcium sulphate bioceramics, Ceram. Int. 31 (2005) 1021–1023.
[4] M.G.-V. Jose, S. Eduardo, P.T. Antoni, O. Takeo, S. Katsuaki, W.M. Grayson, J.M. Sally, Novel bioactive functionally graded coatings on Ti6Al4V, Adv. Mater. 12 (2000) 894–899.
[5] X.Y. Liu, K.C. Paul, C.X. Ding, Surface modification of titanium, titanium alloys, and related materials for biomedical applications, Mater. Sci. Eng. R 47 (2004) 49–121.
[6] Y.C. Yang, E.W. Chang, B.H. Hwang, S.Y. Lee, Biaxial residual stress states of plasma-sprayed hydroxyapatite coatings on titanium alloy substrate, Biomaterials 21 (2000) 1327–1337.
[7] C.F. Feng, K.A. Khor, E.J. Liu, P. Cheang, Phase transformations in plasma sprayed hydroxyapatite coatings, Scripta Mater. 42 (2000) 103–109.
[8] X.B. Zheng, M.H. Huang, C.X. Ding, Bond strength of plasma-sprayed hydroxyapatite/Ti composite coatings, Biomaterials 21 (2000) 841–849.
[9] M.F. Hsieh, L.H. Perng, T.S. Chin, Hydroxyapatite coating on Ti6Al4V alloy using a sol–gel derived precursor, Mater. Chem. Phys. 74 (2002) 245–250.
[10] E. Milella, F. Cosentino, A. Licciulli, C. Massaro, Preparation and characterisation of titania/hydroxyapatite composite coatings obtained by sol–gel process, Biomaterials 22 (2001) 1425–1431.

[11] X.L. Cheng, M. Filiagg, S.G. Roscoe, Electrochemically assisted co-precipitation of protein with calcium phosphate coatings on titanium alloy, Biomaterials 25 (2004) 5395–5403.
[12] Q.Y. Zhang, Y. Leng, R.L. Xin, A comparative study of electrochemical deposition and biomimetic deposition of calcium phosphate on porous titanium, Biomaterials 26 (2005) 2857–2865.
[13] A.L. Yerokhin, X. Nie, A. Leyland, A. Matthews, S.J. Dowey, Plasma electrolysis for surface engineering, Surf. Coat. Tech. 122 (1999) 73–93.
[14] V.M. Frauchiger, F. Schlottig, B. Gasser, M. Textor, Anodic plasma-chemical treatment of CP titanium surfaces for biomedical applications, Biomaterials 25 (2004) 593–606.
[15] L.-H. Li, Y.-M. Kong, H.-W. Kim, Improved biological performance of Ti implants due to surface modification by micro-arc oxidation, Biomaterials 25 (2004) 2867–2875.
[16] W.-H. Song, Y.-K. Jun, Y. Han, S.-H. Hong, Biomimetic apatite coatings on microarc oxidized titania, Biomaterials 25 (2004) 3341–3349.
[17] X.L. Zhu, L.O. Joo, S.Y. Kim, K.H. Kim, Surface characteristics and structure of anodic oxide films containing Ca and P on a titanium implant material, J. Biomed. Mater. Res. 60 (2002) 333–338.
[18] X.L. Zhu, K.-H. Kim, Y.S. Jeong, Anodic oxide films containing Ca and P of titanium biomaterial, Biomaterials 22 (2001) 2199–2206.
[19] F. Liu, F.P. Wang, T. Shimizu, K. Igarashi, L.C. Zhao, Hydroxyapatite formation on oxide films containing Ca and P by hydrothermal treatment, Ceram. Int. 32 (2006) 527–531.
[20] A. Oyane, H.-M. Kim, T. Furuya, T. Kokubo, T. Miyazaki, T. Nakamura, Preparation and assessment of revised simulated body fluids, J. Biomed. Mater. Res. A 65 (2003) 188–195.
[21] S. Koutsopoulos, Synthesis and characterization of hydroxyapatite crystals: a review study on the analytical methods, J. Biomed. Mater. Res. 62 (2002) 600–612.
[22] M. Lenka, A.M. Frank, Preparation of SBF with different HCO_3^- content and its influence on the composition of biomimetic apatites, Acta Biomater. 2 (2006) 181–189.